Spectroelectrochemistry of Poly(ethylenedithiathiophene)−the Sulfur Analogue of Poly(ethylenedioxythiophene)

Antonio Cravino,*,†,‡ Helmut Neugebauer,† Andreas Petr,*,§ Peter J. Skabara,||,⊥ Howard J. Spencer,|| Joseph J. W. McDouall,|| Lothar Dunsch,§ and N. Serdar Sariciftci†

Linz Institute for Organic Solar Cells (LIOS), Physical Chemistry, Johannes Kepler University Linz, 4040 Linz, Austria, Leibniz Institut für Festkoerper- und Werkstoffforschung Dresden, Institut für Festkoerperforschung, Abteilung Elektrochemie und leitfähige Polymere, 01069 Dresden, Germany, and School of Chemistry, University of Manchester, Manchester, United Kingdom

Received: October 28, 2005; In Final Form: December 21, 2005

Poly(3,4-ethylenedithiathiophene) (PEDTT) is a polythiophene-like conjugated polymer in which each thiophene ring is functionalized with an ethylenedithia bridge. As such, PEDTT is the sulfur analogue of the well-known poly(3,4-ethylenedioxythiophene) (PEDOT). Substituent effects, namely the presence of sulfur atoms in PEDTT replacing the oxygen atoms of PEDOT, do not provide a simple explanation for the different electronic properties of the two polymers in the neutral state. This paper reports the spectroscopic properties of PEDTT, studied by in situ techniques such as IR-, Vis-, and electron spin resonance (ESR) spectroelectrochemistry. The differences observed upon electrochemical oxidation of PEDTT and PEDOT (e.g., the different infrared active vibrational band patterns in IR spectroelectrochemistry as well as the different nature of the charged states) are even more marked than those observed in the neutral state. These results, with AM1 calculations, indicate conformational effects as a possible explanation for the different electronic and spectroscopic properties of PEDTT and PEDOT.

Introduction

The well-known poly(3,4-ethylenedioxythiophene) (PEDOT, Figure 1) and its derivatives have been attracting great attention due to their outstanding electronic properties. They are characterized by low energy-gap values, low oxidation potentials, and high electrical conductivity and stability in the oxidized (p-doped) state.[1,2] Water-dispersed p-doped PEDOT (commercially available as Baytron) can be cast as pale blue, almost transparent, thin films with electrical conductivities from 0.05 to 10 S cm^{-1}. Electrochemically deposited and p-doped PEDOT films are transparent and show conductivity up to several hundreds of siemens per centimeter.[1−4] These characteristics make p-doped PEDOT films suitable as electrodes and interfacial hole conducting layers in various types of organic electronic devices, for example, in light emitting diodes, solar cells, and antistatic or electrochromic coatings.[5,6] The outstanding properties of PEDOT can be motivated, in part, by the large mesomeric electron donating effect of the oxygen atoms directly linked to the positions 3 and 4 of the thiophene moiety combined with a relief of steric hindrance as compared to nonannulated poly(3,4-dialkyloxythiopenes).

In the case of poly(3,4-ethylenedithiathiophene) (PEDTT, Figure 1), each thiophene ring is functionalized with an ethylenedithia substituent.[3] As such, PEDTT is the sulfur containing analogue of PEDOT. As compared to the latter, PEDTT shows higher energy gap and oxidation potential. Electrochemically p-doped PEDTT films are dark greenish and show electrical conductivity values lower than those of p-doped PEDOT.[3,4] The presence of sulfur atoms in PEDTT, replacing the oxygen atoms of PEDOT, does not provide a simple explanation for the very different properties of the two polymers. In fact, important electron donating mesomeric effects should also be expected from sulfur, as found for the monomers (EDTT has a lower oxidation potential as compared with EDOT).[1−3] The differences observed upon p-doping the polymeric materials, such as those concerning the vibrational spectra or the different nature of the corresponding charged states, are even more marked. IR spectra of doped or photoexcited conjugated polymers usually are dominated by a few "activated" A_g vibrational bands corresponding to the modes coupled with the π-electron system, that is, those oscillating the conjugated backbone. Thus, a priori, similar patterns for the IR spectra,

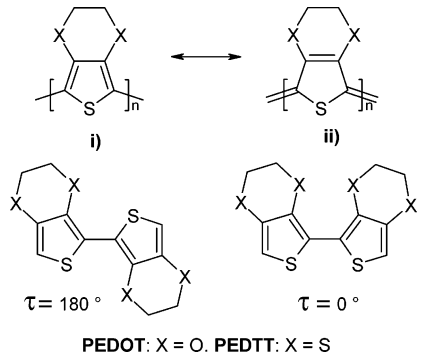

Figure 1. Chemical structures of PEDOT and PEDTT (top) and the corresponding dimers (bottom). Limiting forms: (i) aromatic; (ii) quinoid.

* Corresponding authors. E-mail: antonio.cravino@univ-angers.fr (A.C.); andreas.petr@ifw-dresden.de (A.P.).
† Johannes Kepler University Linz.
‡ Present address: Group Linear Conjugated Systems, CIMMA, CNRS UMR 6200, University of Angers, 49045 Angers CEDEX, France.
§ Abteilung Elektrochemie und leitfähige Polymere.
|| University of Manchester.
⊥ Present address: WestCHEM, Department of Pure and Applied Chemistry, University of Strathclyde, Glasgow G1 1XL, United Kingdom.

10.1021/jp0562173 CCC: $33.50
Published on Web 01/21/2006

not only of the neutral materials but also of the two p-doped or photoexcited polymers, could be expected.

In this work, the spectroscopic behavior of PEDTT upon p-doping has been studied in situ using attenuated total reflection Fourier transform infrared (ATR-FTIR) spectroscopy. The results are compared to those obtained by photoinduced Fourier transform IR absorption (PIA-FTIR) measurements. Visible and near IR (Vis-NIR) electronic absorption and electron spin resonance (ESR) spectra were also recorded, simultaneously and in situ at different doping levels. Different spectroscopic behaviors and features of PEDTT upon p-doping are observed as compared with those of p-doped PEDOT. Geometry optimization performed at the AM1 level suggests that these differences are dictated by the different conformations adopted by the two polymers.

Experimental and Computational Details

Sample Preparation and in Situ ATR-FTIR Spectroelectrochemistry. The monomer EDTT was synthesized according to Goldoni et al.[7] For electropolymerization, the monomer was dissolved in acetonitrile containing 0.1 M tetrabutylammonium hexafluorophosphate as the supporting electrolyte. The solution was then transferred by syringe into the spectroelectrochemical cell. A Ge reflection element covered with an ultrathin layer of evaporated Pt served as the working electrode, while a Pt foil and a Ag/AgCl wire electrode (−190 mV vs saturated calomel electrode (SCE)) were the counter and the quasi-reference electrodes, respectively. The electrochemical equipment consisted of a Jaissle 1002TNC potentiostat, a Prodis 1/14 I sweep generator, and a Rikadenki RY-PIA $x-y$ recorder. After potentiostatic polymerization at the oxidation potential of the monomer, the spectroelectrochemical cell was rinsed with a monomer-free electrolyte solution. Prior to in situ ATR-FTIR spectroelectrochemistry, the polymer films were electrochemically dedoped at −500 mV. The same conditions were used for the preparation of the samples used for photoinduced PIA-FTIR absorption as well as Vis and ESR measurements. To prevent side reactions due to oxygen and/or moisture, all experimental steps were carried out under argon. Doping was performed by cycling the electrochemical potential at a sweep rate of 5 mV s^{-1}. During these cyclic voltammetry experiments, IR spectra were recorded consecutively by means of a Bruker IFS 66S FT spectrophotometer equipped with a liquid nitrogen cooled mercury cadmium telluride (MCT) detector. Each spectrum results from 32 FTIR scans with a resolution of 4 cm^{-1} and covers a range of 85−90 mV in the corresponding cyclic voltammogramm. Spectral changes during p-doping were obtained by referring the actual spectrum to the spectrum recorded at 172 mV. Difference spectra were calculated as $\Delta[-\log T_{ATR}]$, where T_{ATR} is the transmittance in the ATR geometry. The setup used for these experiments was described in detail elsewhere.[8−10]

Photoinduced FTIR Absorption. For PIA-FTIR spectroscopy, samples prepared as described above were mounted on the coldfinger of a liquid nitrogen cooled cryostat with ZnSe windows and were illuminated in 45° geometry. Photoexcitation was achieved by the 488 nm line of an Ar^+ laser, with an impinging light intensity of about 30 mW/cm^2. The PIA-FTIR spectra were obtained by recording 10 single beam spectra under illumination followed by 10 single beam spectra recorded in the dark. Three hundred repetitions of this sequence were accumulated to achieve a better signal-to-noise ratio. The spectra presented were calculated as $-\Delta T/T$.

In Situ Vis-NIR and Electron Spin Resonance Spectroscopy. The polymer films for in situ Vis-ESR investigation were prepared as described above but using an indium tin oxide (ITO) coated glass (Merck, 15 Ω/□) as the working electrode. After polymerization, the films were dedoped electrochemically, rinsed with acetonitrile, and then transferred into the flat cell for in situ ESR measurements described elsewhere.[11] An X-band spectrometer (Bruker ESP300E) was used. All measurements were carried out at room temperature with modulation at 100 kHz and at a microwave power of 2 mW. The cavity Bruker ER 4104 OR resonant in the TE103 mode was used. The Vis-NIR absorption spectra were recorded with a diode array equipped spectrophotometer (J&M, Analytische Mess- und Regeltechnik). During electrochemical potential cycling at a rate of 10 mV s^{-1}, ESR as well as Vis-NIR spectra were recorded consecutively.

Computational Details. The geometries of the dimers in the neutral state ($(EDOT)_2$ and $(EDTT)_2$) and positively charged state ($(EDOT)_2^{\bullet+}$ and $(EDTT)_2^{\bullet+}$) were fully optimized at the level of the semiempirical AM1 Hamiltonian using the Gaussian 98 suite of programs.[12] Following this, a potential surface scan was performed in 10° increments of the dihedral angle between the planes of the rings. The dihedral angle, τ, is defined for the two limiting cases, as shown in Figure 1. For each value of τ, the geometry of the system was fully relaxed with respect to all other geometric variables.

Results and Discussion

In Situ ATR-FTIR Spectroscopy. Because of the electron−phonon interaction in molecules with delocalized π-electron systems, medium IR (MIR) absorption spectra of conjugated polymers in their p-doped or photoexcited states are characterized by a few vibrational bands, named infrared active vibrational (IRAV) bands, accompanied by broad and intense electronic bands.[13−16] While these latter ones correspond to transitions between the electronic levels of paramagnetic radical ions or diamagnetic dications (so-called polarons and bipolarons, respectively) formed by the doping process, the IRAV bands correspond to the A_g modes strongly coupled to the π-electron system as described in several models,[13−16] for example, the effective conjugation coordinate (ECC) theory introduced by Zerbi and co-workers.[15,16] In polyaromatic systems taken as models, ECC is a linear combination of carbon−carbon single and double bond stretching coordinates where the system oscillates between mostly "aromatic" and mostly "quinoid" states (see Figure 1, limiting forms i and ii), which are also the geometries of the ground state and the excited state, respectively.[17] The vibrational modes along these coordinates are those observed in the relatively simple Raman spectra of neutral conjugated polymers and are normally IR inactive. However, when charges are injected onto the chain by doping processes, these modes are IR-activated by the breakdown of local symmetry around the charged sites. The corresponding IRAV bands are therefore related to the extension of the electron delocalization along the quasi-one-dimensional pattern of alternating C−C single and double bonds in π-conjugated systems. As such, due to the different electronic properties of PEDTT and PEDOT, mainly the energy-gap value, the absolute position of their IRAV bands might be expected to be different in the corresponding spectra. However, despite the topological similarity of PEDOT and PEDTT, differences are also found concerning the *number of main* IRAV bands as well as their behavior with increasing electrochemical potential, that is, increasing doping level.

The IR difference spectra recorded in situ upon electrochemical p-doping of PEDTT are depicted in Figure 2a. Four IRAV

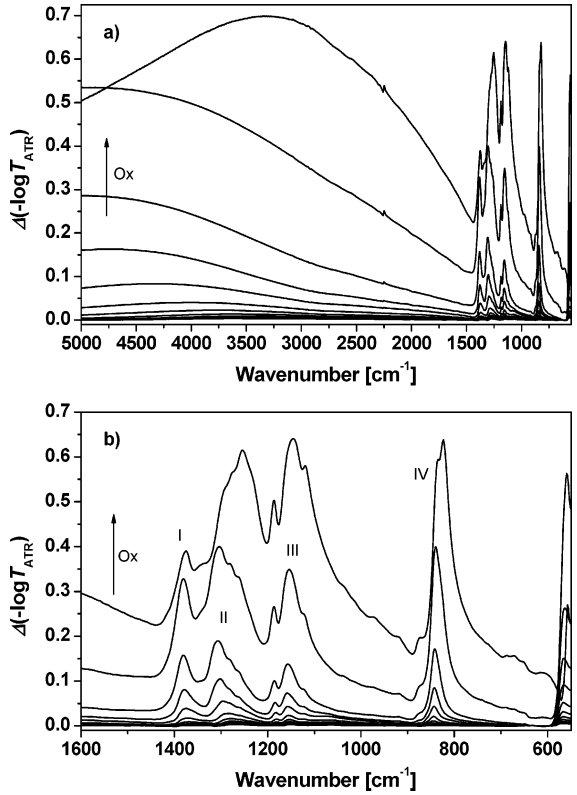

Figure 2. IR difference spectra of PEDTT films recorded during electrochemical oxidation (p-doping). Sequence: bottom to top. (a) Extended range; (b) IRAV range.

TABLE 1: IRAV Bands of Oxidized (p-Doped) and Photoexcited PEDTT[a]

E vs SCE (mV)	I	II	III	IV
1200	1375	1253	1145	825
1115	1381	1304	1153	840
1030	1381	1307	1157	843
945	1379	1302	1159	843
860	1375	1296	1157	843
775	1371	1282	1155	845
690	1369	1279	1153	845
605	1367	1275	1153	845
520	1367	1273	1153	847
435	1365	1271	1151	848
PIA	1381	1302	1149	837

[a] The position of the bands is given in wavenumbers (cm^{-1}). PIA refers to the photoinduced (488 nm as the excitation wavelength) IRAV bands.

bands and an electronic absorption band develop with increasing electrochemical potential. The positions of the IRAV bands are collated in Table 1, along with those derived from the PIA-FTIR spectrum. The results are in agreement with the data reported by Wang and co-workers.[3] However, the in situ experiment shows that most features undergo significant shifts with increasing doping levels. At the beginning of the oxidation process (electrochemical potential of up to ~700 mV), the broad doping-induced electronic absorption band has a maximum at about 4000 cm^{-1}. Increasing the potential to ~1000 mV results in a shift of this maximum to a value >5000 cm^{-1}. Finally, when the potential reaches 1200 mV, a maximum is clearly seen at 3285 cm^{-1}. The first shift to higher wavenumbers can be assigned, tentatively, to the progressive oxidation of chain segments with shorter effective conjugation length (i.e., with higher oxidation potential) having a higher band gap and therefore an increased separation between the "valence band" edge and the doping-induced level(s). The subsequent red shift might be motivated by the attainment of a heavily doped state with increased quinoid character, thus leading to a higher in-chain delocalization of the charged states.

Contrary to PEDOT (and other conjugated polymers),[18−25] the IRAV bands of PEDTT undergo clear frequency shifts with increasing doping level, too. Such a frequency dispersion upon electrochemical doping was reported also for poly(3,4-dioctyloxythiophene) (PDOT)[26] and poly(benzo[*c*]thiophene).[27] This behavior is not common. In other conjugated polymers and as far as reversible processes are involved, increasing the anodic polarization potential mainly, if not solely, causes an increase of the IRAV bands' intensity without an important shift of their position.[18−25] In PEDTT, as already seen for the electronic transition band, first there is a shift to higher wavenumbers, followed by a clear and predominant shift to lower values when the electrochemical potential increases (Figure 2b and Table 1). In particular, a relevant shift can be seen for band II: its frequency dispersion spans the range from well above 1310 cm^{-1} to 1257 cm^{-1} (overall shift of 53 cm^{-1}). The last value could even be attributed to a new band, indicative of a high doping level, since a developing shoulder at this position can be noted in the spectra recorded at lower electrochemical potentials (Figure 2b). Conversely, a high energy side shoulder is seen for this new band, at a wavenumber of about 1300 cm^{-1}. Bands I and III show the same behavior; the spanned wavenumber range is limited to 16 and 14 cm^{-1}, respectively. The narrow and intense peak at 836−840 cm^{-1} due to the incorporation of hexafluorophosphate counterions overlaps a genuine feature of doped PEDDT, as described by Wang and co-workers[3] and confirmed by the PIA absorption spectrum in the next subsection.

To explain the shift of the bands described above with the formation of bipolarons after the polarons was proposed by Szkurlat et al., who have described the behavior of PDOT.[26] However, for PEDTT, this interpretation is not consistent with the ESR results discussed in the following. A link between the position of IRAV and electronic bands in doped conjugated polymers has been proposed by Ehrenfreund and Vardeny.[28] This model might explain the observed PEDTT's behavior.

Photoinduced IR Absorption. Figure 3 shows the PIA-FTIR spectrum of PEDTT. Excitation was carried out at 488 nm, within the polymer electronic absorption band.[3] The observation of an IRAV pattern indicates photoinduced charge generation in pristine PEDTT. In the photoexcited case, electronic transitions are seen by the broad band extending from ~2000 to ~5000 cm^{-1} or above (see Figure 3a). According to Wang et al.[3] and as mentioned before, the observation of a photoinduced IRAV band at about 837 cm^{-1} leads to the conclusion that in the electrochemical case this feature is indeed present and overlaps the counterion band. The vibrational part of the PIA spectrum (Figure 3b) resembles that of the spectrum recorded at a high doping level (1115 mV) in the electrochemical case.

In Situ Vis-NIR and ESR Spectroscopy. Figure 4 shows the cyclic voltammogram of a PEDTT film on ITO. During cyclic voltammetric experiments, 11 ESR spectra and 20 Vis-NIR spectra were recorded at equidistant potential steps. The ESR spectra, as shown in Figure 5, are almost insensitive to electrochemical potential changes. A very low signal-to-noise ratio, as already pointed out by Wang et al.,[3] indicates a very low concentration of paramagnetic species, independent of the electrochemical potential applied. This is unusual for rather thick and electrochemically polymerized samples. Indeed, in many other electrochemically prepared conjugated polymers, a much

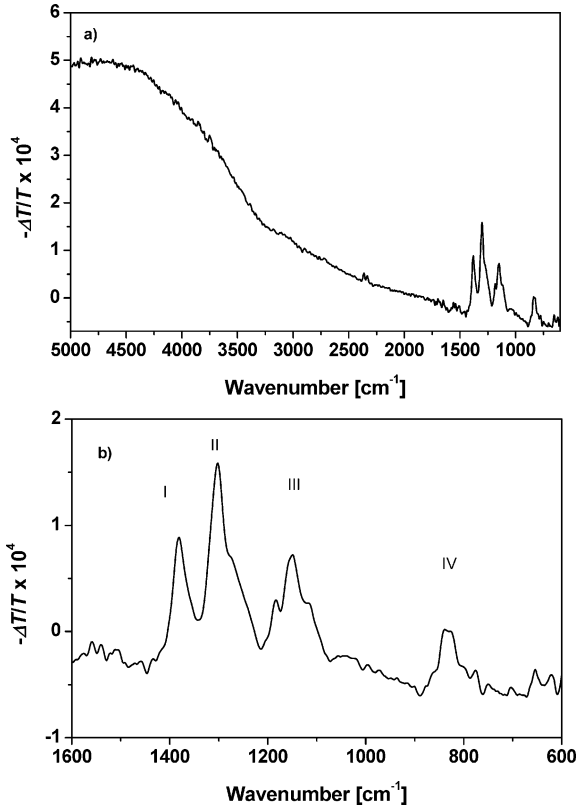

Figure 3. PIA-FTIR spectrum of PEDTT. Excitation at 488 nm. (a) Extended range; (b) IRAV range.

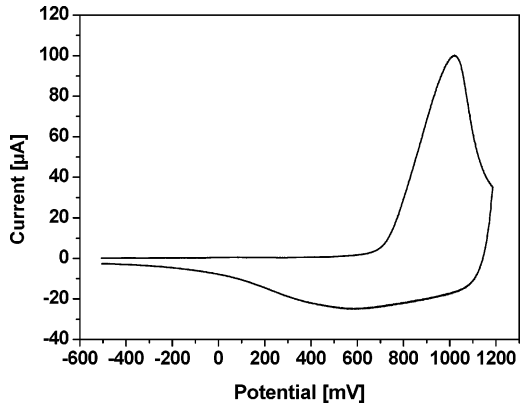

Figure 4. Cyclic voltammogram recorded in situ during the UV−Vis-NIR and ESR spectroelectrochemical experiment.

larger concentration of residual polarons can be detected in their "neutralized" form. In PEDTT, the low number of spins in the neutral state (cathodic potential of −500 mV) even decreases upon p-doping. Accordingly, absorption bands related to the formation of paramagnetic species as polarons are not observed in the Vis-NIR spectra. These latter are shown in two sequences. Figure 6a displays the first 10 Vis-NIR spectra. This ensemble of spectra, with an isosbestic point at 920 nm, clearly indicates the formation of an oxidized product absorbing at ∼1350 nm. At the beginning of the process, two feeble negative features can be seen at about 800 and 1550 nm. In accordance with the ESR measurements, this bleaching can be assigned to the oxidation of residual polarons to bipolarons. Increasing the potential, the growth of a single broad absorption band clearly indicates the further formation of bipolarons. It can be noted that the bleaching of the $\pi-\pi^*$ absorption occurs only for the longest conjugated segments of the chain, as indicated by the negative bands centered around 600 nm. In PEDOT, instead,

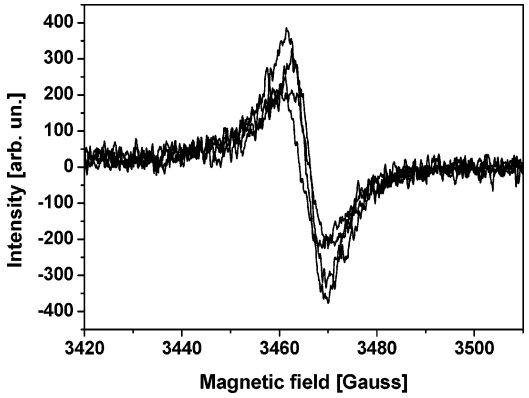

Figure 5. ESR spectra of PEDTT recorded during electrochemical oxidation (p-doping). The spectra displayed are those recorded at −500 mV (start and end of the electrochemical potential swap), +520 mV, and 1200 mV (higher electrochemical potential reached in the experiments, lowest ESR signal).

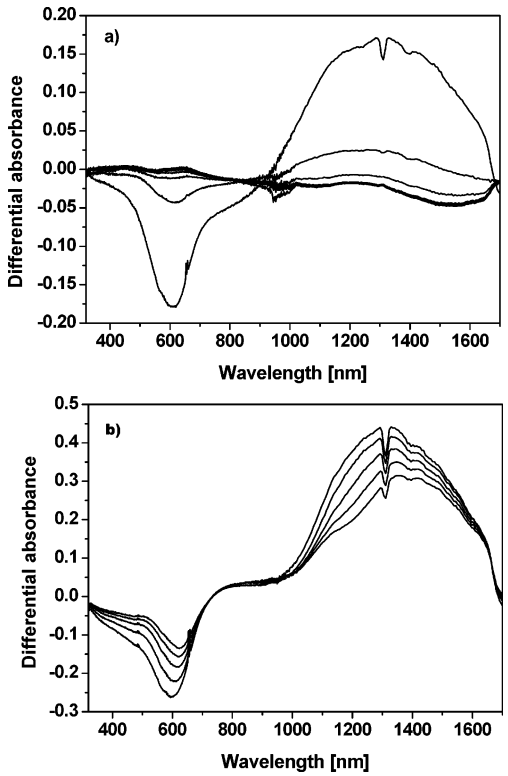

Figure 6. Vis-NIR absorption spectra of PEDTT during electrochemical oxidation (p-doping) and re-reduction: (a) oxidation, bottom −500 mV, top ∼1200 mV; (b) re-reduction, top 216 mV, bottom −500 mV.

the entire distribution of conjugation lengths is affected by doping.[29] As can be seen in Figure 6b, and according to the cyclic voltammogram (CV) trace, a complete re-reduction was not achieved during the spectroelectrochemical experiments. PEDTT films recovered their neutral state only after about 10 min at an applied potential of −500 mV. These results are indicative of very different kinetics for the doping/dedoping processes.

Comparison between p-Doped PEDTT and p-Doped PEDOT. *Vibrational and Conformational Properties.* The IR spectroelectrochemical properties of PEDTT are very different as compared with those of PEDOT. Since IRAV bands are related to a few "selected" modes vibrating along the conjugated pattern, in topologically equivalent conjugated systems, differences should be limited to bandwidth, position, and intensity, rather than affecting the overall number of IRAV bands and

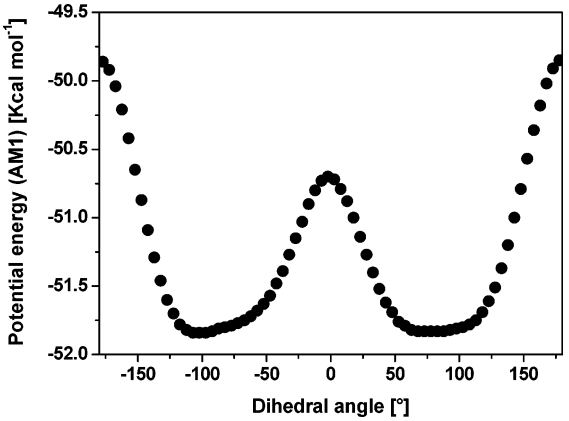

Figure 7. Potential curve (AM1) for rotation about the inter-ring bond in $(EDOT)_2$.

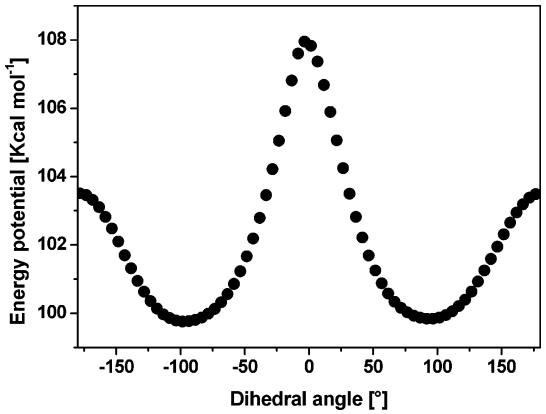

Figure 8. Potential curve (AM1) for rotation about the inter-ring bond in $(EDTT)_2$.

the general pattern of the spectrum. The clear difference observed between the spectra of p-doped PEDTT and PEDOT (the spectrum of the latter is shown in the Supporting Information) is therefore not straightforward. In the case of PEDOT, at least six bands are clearly observed, and the IRAV pattern is more convoluted.

These results suggest that, despite having the same topological structures, the two polymers should belong to different symmetry groups. Therefore, it seems that conformational or solid-state effects play an important role in determining the properties of the two materials. Here, it is important to recall that S···S and S···O interactions are known to drive the conformation of thiophene based oligomers containing ethylenechalcogeno groups.[30−32] To gain some insight into the conformational behavior of PEDTT and PEDOT, calculations were performed on the corresponding neutral and positively charged dimers. In $(EDOT)_2$, the potential curve for rotation about the inter-ring bond has been found to be very flat, with a barrier of only about 1 kcal mol^{-1} for $\tau = 0°$ and 2 kcal mol^{-1} for $\tau = 180°$ (see Figure 7). The minimum in the potential energy occurs when τ equates to 73°. In $(EDTT)_2$, the conformation with the minimum energy is more twisted and occurs at $\tau = 92°$. The energy barriers for rotating through $\tau = 0°$ and $\tau = 180°$ are 8 and 4 kcal mol^{-1}, respectively (Figure 8). While this work was ongoing, Hong has performed periodic AM1 calculations and has found barriers for rotation through 180° for PEDOT of approximately 2 kcal mol^{-1}, while for PEDTT the barrier was approximately 4 kcal mol^{-1}.[4] These results indicate that the conformation of PEDOT, though rather planar and favoring electron delocalization, might be characterized by torsional angles which gradually span a *relatively* wide range around the potential minimum's value. In contrast, as indicated by the potential energy profile found for $(EDTT)_2$, PEDTT should have, *although more twisted*, a more rigid chain, that is, a more defined conformation, and, thus, a higher degree of symmetry. To consider the charged states, calculations on $(EDOT)_2^{\bullet+}$ and $(EDTT)_2^{\bullet+}$ were performed. Introducing a positive charge on the dimers results in less pronounced differences. For both dimers, stable conformations were found at $\tau = 180°$ (see the Supporting Information and ref 4). Thus, opposite to the neutral state, the charged polymer segments should have a similar conformation.

The results presented in the ESR subsection show that bipolarons are directly formed upon p-doping of PEDTT. In PEDOT, contrary to PEDTT, equilibrium between polarons and bipolarons is observed.[33] This difference can also be explained by the different conformations of the two polymers. In PEDOT, its planar conformation and the substituent electronic effects play a synergistic role, resulting in a low energy gap and a low oxidation potential. Doping of PEDOT can be achieved at about 0 mV. Beginning the doping process results in polaron formation, followed by that of bipolarons at higher electrochemical potentials. In PEDTT, the electronic effects of the sulfur atoms are suppressed by the twisted chain's conformation, which hinders electron delocalization and therefore increases the energy-gap and the oxidation potential values. As such, doping of PEDTT starts only at higher potentials, in a range in which bipolarons are already formed in PEDOT. After the formation of a polaron, the charged chain's segment should adopt a more planar conformation. This conformational change dramatically reduces the difference between PEDOT and PEDTT. As such, at the considered potentials, the formed polaron should immediately undergo a second oxidative step, leading to a bipolaron, explaining why no polaron formation is observed upon PEDTT's doping. Thus, a strong interplay between geometrical factors and electronic/electrochemical properties, similar to that observed with some small and well-defined molecules (e.g., in tetracyanoquinodimethane, a two-electron process leads directly to dianions),[34] can be proposed for PEDTT, too. In addition, this mechanism can explain the different kinetics of the doping/dedoping processes and does not prevent the observation of residual polarons in re-reduced PEDTT samples.

Conclusions

In this paper, we report the properties of p-doped PEDTT, as investigated by in situ techniques such as ATR-FTIR, Vis-NIR, and ESR spectroelectrochemistry. Despite the topological equivalence of PEDTT and PEDOT, their IRAV signatures are found to be different. These results, with those derived by semiempirical calculations, suggest very different conformations for the two materials. This difference may also explain the rather unusual case of PEDTT, for which no polaron formation is observed upon electrochemical p-doping.

Acknowledgment. We thank Pierre Frère for valuable discussions.

Supporting Information Available: Difference FTIR absorbance spectra of PEDOT recorded during electrochemical oxidation and potential energy profiles for $(EDOT)_2^{\bullet+}$ and $(EDTT)_2^{\bullet+}$. This material is available free of charge via the Internet at http://pubs.acs.org.

References and Notes

(1) Heuer, H. W.; Whermann, R.; Kirchmeyer, S. *Adv. Funct. Mater.* **2002**, *12*, 89.

(2) Kirchmeyer, S.; Reuter, K. *J. Mater. Chem.* **2005**, *15*, 2077.
(3) Wang, C.; Schindler, J. L.; Kannewurf, C. R.; Kanatzidis, M. G. *Chem. Mater*. **1995**, *7*, 58.
(4) Hong, S. Y. *Synth. Met*. **2003**, *135*−*136*, 439.
(5) Brabec, C. J.; Sariciftci, N. S.; Hummelen, J. C. *Adv. Funct. Mater*. **2001**, *11*, 15.
(6) Burroughes, J. H.; Bradley, D. D. C.; Brown, A. R.; Marks, R. N.; Mackay, K.; Friend, R. H.; Burns, P. L.; Holmes, A. B. *Nature* **1990**, *347*, 539.
(7) Goldoni, F.; Langeveld-Voss, B. M. W.; Meijer, E. W. *Synth. Commun.* **1998**, *28*, 2237.
(8) Neugebauer, H.; Sariciftci, N. S. In *Lower Dimensional Systems and Molecular Electronics*; Metzger, R. M., Day, P., Papavassiliou, G. C., Eds.; Nato ASI series, Series B: Physics, Vol. 248; Plenum Press: New York, 1991; p 401.
(9) Neugebauer, H. *Macromol. Symp*. **1995**, *94*, 61.
(10) Kvarnström, C.; Neugebauer, H.; Ivaska, A. In *Advanced Functional Molecules and Polymers*; Nalwa, H. S., Ed.; Gordon & Breach: Langhorne, PA, 2001; Vol. 2, Chapter 3.
(11) Dunsch, L.; Petr, A. *Ber. Bunsen-Ges. Phys. Chem.* **1993**, *97*, 436.
(12) Frisch, M. J.; Trucks, G. W.; Schlegel, H. B.; Scuseria, G. E.; Robb, M. A.; Cheeseman, J. R.; Zakrzewski, V. G.; Montgomery, J. A., Jr.; Stratmann, R. E.; Burant, J. C.; Dapprich, S.; Millam, J. M.; Daniels, A. D.; Kudin, K. N.; Strain, M. C.; Farkas, O.; Tomasi, J.; Barone, V.; Cossi, M.; Cammi, R.; Mennucci, B.; Pomelli, C.; Adamo, C.; Clifford, S.; Ochterski, J.; Petersson, G. A.; Ayala, P. Y.; Cui, Q.; Morokuma, K.; Malick, D. K.; Rabuck, A. D.; Raghavachari, K.; Foresman, J. B.; Cioslowski, J.; Ortiz, J. V.; Stefanov, B. B.; Liu, G.; Liashenko, A.; Piskorz, P.; Komaromi, I.; Gomperts, R.; Martin, R. L.; Fox, D. J.; Keith, T.; Al-Laham, M. A.; Peng, C. Y.; Nanayakkara, A.; Gonzalez, C.; Challacombe, M.; Gill, P. M. W.; Johnson, B. G.; Chen, W.; Wong, M. W.; Andres, J. L.; Head-Gordon, M.; Replogle, E. S.; Pople, J. A. *Gaussian 98*, revision A.11.3; Gaussian, Inc.: Pittsburgh, PA, 1998.
(13) Horovitz, B. *Solid State Commun.* **1982**, *41*, 729.
(14) Ehrenfreund, E.; Vardeny, Z. V.; Brafman, O.; Horowitz, B. *Phys. Rev. B* **1987**, *36*, 1535.
(15) Castiglioni, C.; Gussoni, M.; Lopez Navarrete, J. T.; Zerbi, G. *Solid State Commun.* **1988**, *36*, 1535.
(16) Zerbi, G.; Gussoni, M.; Castiglioni, C. In *Conjugated Polymers*; Bredas, J. L., Silbey, R., Eds.; Kluwer: Dordrecht, The Netherlands, 1991; p 435.
(17) This applies to most of the reported conjugated polymers, such as polythiophenes, polyphenylenes, poly-*para*-phenylenevinylenes, and polydithienothiophenes. In cases like polyisothianaphtene, the situation can be reversed.
(18) Cravino, A.; Neugebauer, H.; Luzzati, S.; Catellani, M.; Petr, A.; Dunsch, L.; Sariciftci, N. S. *J. Phys. Chem. B* **2002**, *106*, 3583.
(19) Cravino, A.; Neugebauer, H.; Luzzati, S.; Catellani, M.; Sariciftci, N. S. *J. Phys. Chem. B* **2001**, *105*, 46.
(20) Kvarnström, C.; Neugebauer, H.; Blomquist, S.; Ahonen, H. J.; Kankare, J.; Ivaska, A.; Sariciftci, N. S. *Synth. Met*. **1999**, *101*, 66.
(21) Neugebauer, H.; Kvarnström, C.; Cravino, A.; Yohannes, T.; Sariciftci, N. S. *Synth. Met*. **2001**, *116*, 115.
(22) Kvarnstrom, C.; Neugebauer, H.; Ivaska, A.; Sariciftci, N. S. *J. Mol. Struct*. **2000**, *521*, 271.
(23) Pohjakallio, M.; Sundholm, G.; Talonen, P. *J. Electroanal. Chem*. **1996**, *406*, 165.
(24) Khim, Y. H.; Hotta, S.; Heeger, A. J. *Phys. Rev. B* **1987**, *36*, 7486.
(25) Kuzmany, H.; Sariciftci, N. S.; Neugebauer, H.; Neckel, A. *Phys. Rev. Lett*. **1988**, *60*, 212.
(26) Szkurlat, A.; Palys, B.; Mieczkowski, J.; Skompska, M. *Electrochim. Acta* **2003**, *48*, 3665.
(27) Jones, C. L.; Higgins, S. J.; Christensen, P. A. *J. Mater. Chem*. **2002**, *12*, 758.
(28) Ehrenfreund, E.; Vardeny, Z. V. *Proc. SPIEE* **1997**, *3145*, 324.
(29) Kvarnström, C.; Neugebauer, H.; Blomquist, S.; Ahonenc, H. J.; Kankare, J.; Ivaska, A. *Electrochim. Acta* **1999**, *44*, 2739.
(30) Pozo-Gonzalo, C.; Khan, T.; McDouall, J. J. W.; Skabara, P. J.; Roberts, D. M.; Light, M. E.; Coles, M. J.; Hursthouse, M. B.; Neugebauer, H.; Cravino, A.; Sariciftci, N. S. *J. Mater. Chem*. **2002**, *12*, 500.
(31) Spencer, H. J.; Skabara, P. J.; Giles, M.; McCulloch, I.; Coles, S. J.; Hursthouse, M. B. *J. Mater. Chem.* **2005**, *15*, 4783.
(32) Turbiez, M.; Frère, P.; Allain, M.; Gallego-Planas, N.; Roncali, J. *Macromolecules* **2005**, *38*, 6806.
(33) Xu-Sheng, D.; Ping-Ping, S.; Zheng-Hao, W. *Huaxue Xuebao* **2003**, *61*, 536.
(34) Kini, A. M.; Cowan, D. O.; Gerson, F.; Möckel, R. J. *J. Am. Chem. Soc.* **1985**, *107*, 556.